2004

Construction of a MIMO testbed for space time block codes

Albert J. Davis
Lehigh University

Davis, Albert J

Construction of a MIMO Testbed for Space Time Block Codes

September 2004

Construction of a MIMO Testbed for Space Time Block Codes

By

Albert J Davis

A Thesis
Presented to the Graduate and Research Committee
Of Lehigh University
In Candidacy for the Degree of
Master of Science

In
Electrical Engineering

Lehigh University
August 2004

This thesis is accepted and approved in partial fulfillment of the requirements for the Master of Science

8-12-04

Date

Thesis Advisor

Chairperson of Department

Table Of Contents

Table of Figures

I. Abstract

A hardware platform is desired to fully explore the details of implementation for Multiple Input Multiple Output (MIMO) schemes like Alamouti's Space Time Block Code (STBC). While it is possible to study the performance of these algorithms in simulation, the assumptions inherent to the simulation mean that the algorithm's performance when applied to a real system may not match the expected behavior. Most researchers assume ideal timing and phase tracking at the receiver as well as a perfect channel estimation process for their simulations. In practical systems, however, these assumptions are not realistic. In order to explore the multiple aspects of MIMO, this research testbed was created to demonstrate a platform that allows the evaluation of the MIMO channel and implement space-time algorithms like Alamouti's STBC that can take advantage of the system's MIMO architecture.

II. Introduction

This paper presents Alamouti's theoretical Space Time Block Code (STBC) equations and describes a Multiple Input Multiple Output (MIMO) Antenna testbed that has been built to demonstrate the implementation and effectiveness of these equations. The RF system design and preliminary recorded data will be presented at the end of this paper. The recorded data from the testbed has been analyzed and evaluated to show the gains of the MIMO channel and it's capacity.

III. Alamouti's Space Time Block Code

In order to understand the gains associated with Alamouti's Space Time Block Code, a brief review of Maximal Ratio Receive Combining (MRRC) is needed.

A. Maximal Ratio Receive Combining:

Consider a 1x2 Single Input Multiple Output (SIMO) transceiver system shown in Figure 1. In this scheme the symbol transmitted at any given time is received at both the antennas after going through two different and independent channels. The two channels between transmit antenna one and both receive antenna one and two are denoted by h_{11} and h_{12} respectively.

$$h_{11} = \alpha_{11} e^{j\theta_{11}} \quad (1.1)$$

$$h_{12} = \alpha_{12} e^{j\theta_{12}} \quad (1.2)$$

Here α_{11} and α_{12} are magnitudes of the fading coefficients which each have a Rayleigh distribution. The angles of the fading coefficients θ_{11} and θ_{12} are assumed to be uniformly distributed between 0 to 360 degrees. Noise and interference is added at the receiver antennas as given by n_1 and n_2 respectively for antenna 1 and 2, which are Gaussian distributed.

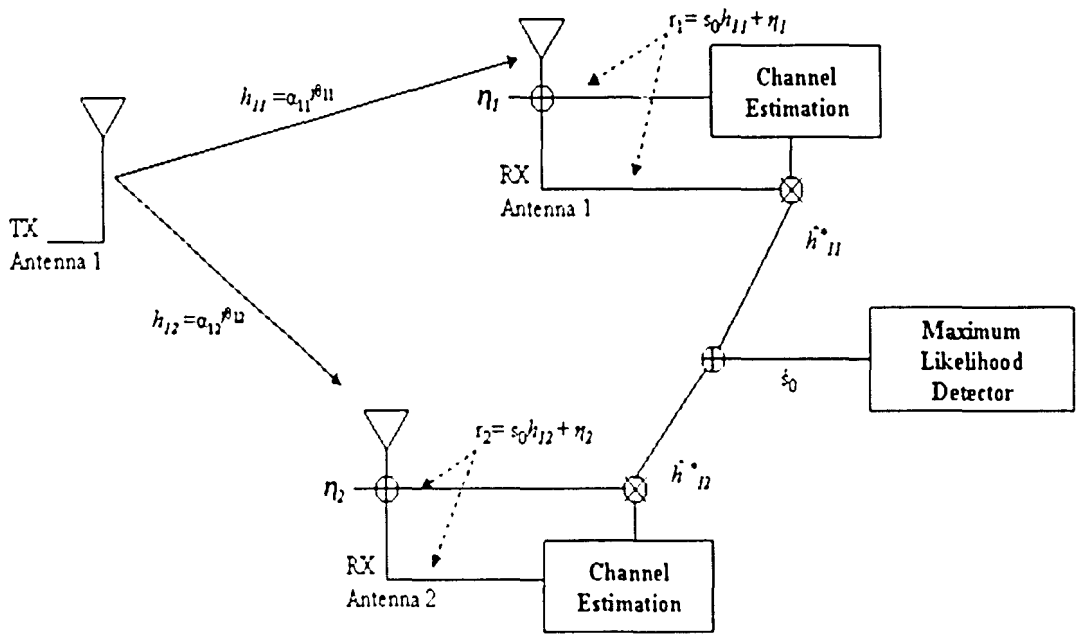

Figure 1: Example of a MRRC scheme.

The received signals are:

$$r_1 = s_0 h_{11} + n_1 \quad (1.3)$$

and

$$r_2 = s_0 h_{12} + n_2. \quad (1.4)$$

At the receiver each antenna has a channel estimator which estimates the values of h_{11} and h_{12} as ($\hat{h}_{11}$ and $\hat{h}_{12}$) with the help of the orthogonal pilot symbols. These estimates are

then fed to the MRRC scheme given below to develop a better projection of the transmitted signal as

$$\tilde{s}_0 = \hat{h}_{11}^{*} r_1 + \hat{h}_{12}^{*} r_2 \quad . (1.5)$$

Maximum likelihood detection follows the combining operation in order to determine the signal that was transmitted. This is done by making a decision on the symbol s_0 where i is the minimum Euclidian distance between $\hat{s}_0$ and a known symbol from the transmitted symbol set given [2] as

$$i = \min_k \left[d^2 (\tilde{s}_0, s_k) \right] \quad .$$

B. Coherent Space Time Block Coding:

Space-Time Block Coding is a simple transmit diversity scheme that achieves the same diversity advantage of Maximal Ratio Receive Combining. Figure 2 shows a 2x1 Multiple Input Single Output (MISO) antenna system, which uses space-time block coding on the data sequence to be transmitted. The receiver uses a combining scheme followed by maximum likelihood detection. This is described in detail next.

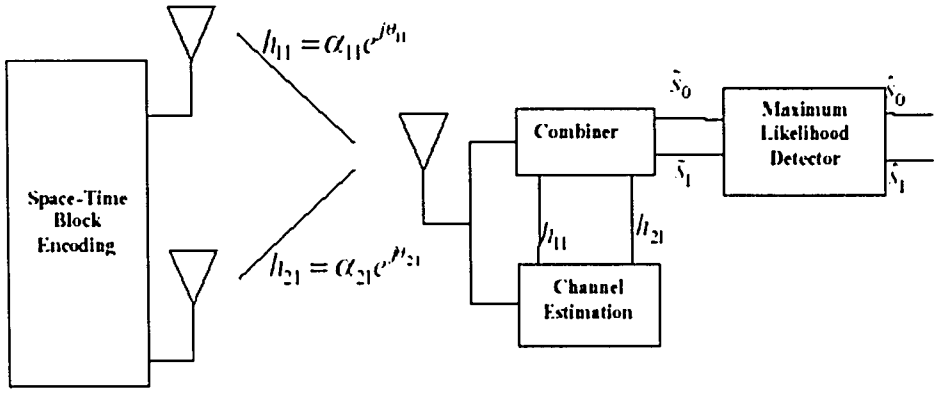

Figure 2: Space-time block coding for 2x1 MISO channel

The transmitted sequence of symbols is coded in such a way as to form a space time block as shown in Figure 3. At time t symbol s_0 is transmitted from antenna one and s_1 is transmitted from antenna two. In the next symbol duration $-s_1^*$ is transmitted from antenna one and s_0^* is transmitted from antenna two. It can be seen that the space-time block coding matrix is orthogonal. The channel between the first transmit antenna and the first receive antenna is represented by h_{11} and between the second transmit antenna and the first receive antenna is represented by h_{21} where

$$h_{11} = \alpha_{11} e^{j\theta_{11}} \quad (17)$$

and

$$h_{21} = \alpha_{21} e^{j\theta_{21}} \quad (18)$$

Space

Time

	Transmit Antenna 1	Transmit Antenna 2
Time t	s_0	s_1
Time t+T	$-s_1^*$	s_0^*

Figure 3: Space-time block coding on source symbol sequence (S0, S1)

Here the channel is assumed to be static across two consecutive symbols and n_1 and n_2 are complex random variables representing noise and interference. Therefore the received signal can be expressed as

$$r_1 = r(t) = s_0 h_{11} + s_1 h_{21} + \eta_1 \quad (1.9)$$

and

$$r_2 = r(t+T) = -s_1^* h_{11} + s_0^* h_{21} + \eta_2 . \quad (1.10)$$

For the combining process at the receiver, the signal received is typically assumed to be coherent and the channel estimation is perfect. Hence the combining scheme used is described by

$$\hat{s}_0 = \hat{h}_{11}^* r_1 + \hat{h}_{21} r_2^* = \alpha_{11}^2 s_0 + \alpha_{21}^2 s_0 + n_1 \hat{h}_{11}^* + n_2^* \hat{h}_{21} \quad (1.11)$$

$$\hat{s}_1 = \hat{h}_{21}^* r_1 - \hat{h}_{11} r_2^* = \alpha_{21}^2 s_1 + \alpha_{11}^2 s_1 + n_1 \hat{h}_{21}^* - n_2^* \hat{h}_{11} \quad (1.12)$$

It can be seen that the first two terms are magnitudes of the fade coefficients and the last two terms are noise terms, which are small.

Maximum likelihood detection follows the combining scheme to determine the signals s_0 and s_1 from the transmitted projections in 1.11 and 1.12. The maximum likelihood equation was described above in equation 1.6. It can be seen that the combining scheme is different from the MRRC scheme but the diversity advantage remains the same. Now we expand the analysis to a 2x2 MIMO system as shown in Figure 4. In this figure the received signals at time t are given by equation 1.13 and 1.14 as

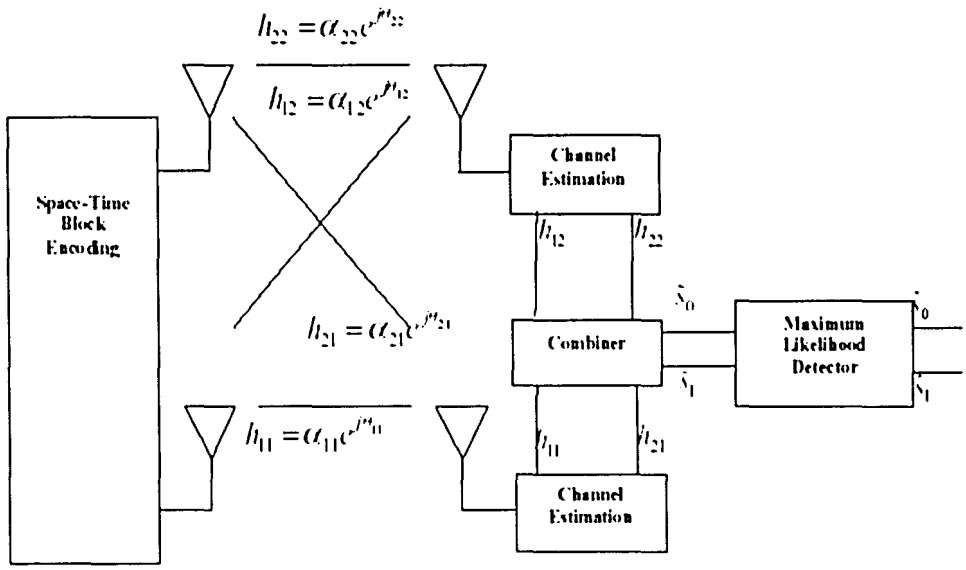

Figure 4: Block diagram of 2x2 MIMO STBC scheme.

$$r_1 = s_0 h_{11} + s_1 h_{21} + n_1 \quad \text{(at receive antenna one)}$$
$$\text{and} \qquad (1.13)$$
$$r_2 = s_0 h_{12} + s_1 h_{22} + n_2 \quad \text{(at receive antenna two)}$$
$$. \qquad (1.14)$$

The signals received at time $t + T$ are given by equation 1.15 and 1.16.

$$r_3 = -s_1^* h_{11} + s_0^* h_{21} + n_3 \quad \text{(at receive antenna one)} \qquad (1.15)$$
$$\text{and}$$
$$r_4 = -s_1^* h_{12} + s_0^* h_{22} + n_4 \quad \text{(at receive antenna two)}. \qquad (1.16)$$

Here n_1, n_2, n_3 and n_4 are complex Gaussian random variables representing noise and interference. Now the combining scheme for the received signals to achieve the diversity advantage is given by

$$\tilde{s}_0 = \hat{h}_{11}^* r_1 + \hat{h}_{21} r_2^* + \hat{h}_{12}^* r_3 + \hat{h}_{22} r_4^* = (\alpha_{11}^2 + \alpha_{21}^2 + \alpha_{12}^2 + \alpha_{22}^2) s_0 + n_1 \hat{h}_{11}^* + n_2 \hat{h}_{12}^* + n_3^* \hat{h}_{21} + n_4^* \hat{h}_{22} \quad (1.17)$$

and

$$\tilde{s}_1 = \hat{h}_{21}^* r_1 - \hat{h}_{11} r_2^* + \hat{h}_{22}^* r_3 - \hat{h}_{12} r_4^* = (\alpha_{11}^2 + \alpha_{12}^2 + \alpha_{21}^2 + \alpha_{22}^2) s_1 + n_1 \hat{h}_{21}^* + n_2 \hat{h}_{22}^* - n_3^* \hat{h}_{11} - n_4^* \hat{h}_{12}. \quad (1.18)$$

The output of the combining scheme is fed to the maximum likelihood detector where a decision is made based on equation 1.6. The advantage of using a 2x2 system is that the diversity order has increased by 4. Figure 5 shows the simulation results for the bit error rate (BER) performance of the coherent STBC scheme compared to MRRC scheme. In these theoretical simulations the total transmitted power for the case with STBC is assumed to be equal to the transmitted power of single transmit power element case with MRRC. Hence there is a degradation in performance in the case of transmit diversity when compared to the same order of receive diversity with MRRC, as the received signal power from each transmit antenna in MRRC scheme is larger than the transmit diversity case. The channels for the MIMO case are assumed to be mutually uncorrelated and undergoing Rayleigh fading. Also the perfect knowledge of channel state information (CSI) at the receiver is assumed in this theoretical simulation.

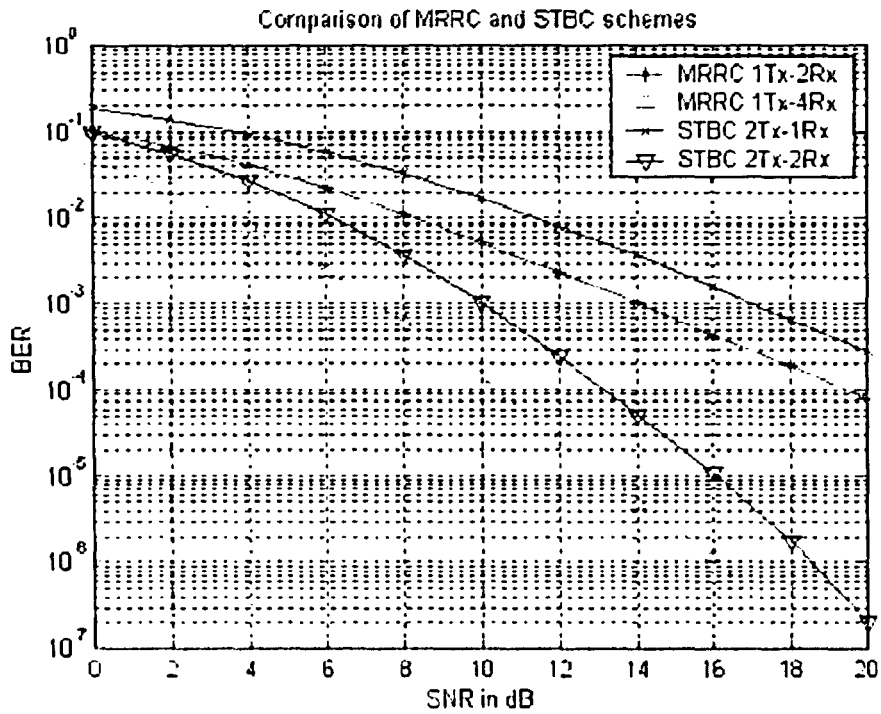

Figure 5: BER Vs SNR of MRRC and STBC schemes

The performance of coherent STBC scheme depends on the perfect channel estimation and carrier recovery. Throughout the construction of this testbed, the hardest part in building a MIMO receiver was estimating the channel response dealing with timing and carrier offsets. In order to accurately measure these parameters long sequences of pilot symbols were inserted frequently in the transmitted data frame. This approach yields better bit error rates but comes at a cost of giving up data throughput.

IV. System Design

The goal of this testbed program was to build a (2x2) MIMO receiver out of existing RF hardware modules that could be software controlled and interfaced into Matlab. Comblock was chosen as the vender for these modules because they provided separate

software controlled RF modules that could form a single RF transmit and receive chain. The modules can also share a single clock input in order to improve synchronization between the two modules that make up the (2x2) MIMO transmit or receive configurations. The first test of this system was to correctly transmit orthogonal pilot symbols and Space Time Block Coded data out of the MIMO transmitter and receive them at the MIMO receiver. The following sections will describe the operation and design of the testbed.

A. Automatic Frequency Compensation

An automatic frequency compensation (AFC) circuit is usually employed to coarsely compensate for the carrier offset. After the frequency compensation from the coarse AFC circuit, a residual frequency offset on the order of 0.1ppm will still exist on the baseband signal. This residual offset is usually handled within the channel estimation algorithms described below. The following formula is the sampled signal from the baseband demodulator. The symbol θ is the unknown random phase, Δf is the unknown carrier frequency and Ts is the sampling period. Thus the receiver's baseband signal can be modeled as

$$r_k = e^{j(2\pi \Delta\tilde{f}\ kTs + \theta)} \quad (1.19)$$

Essentially to estimate the frequency offset we are led to the problem of seeking the maximum of the equivalent likelihood function [2].

$$\Lambda(\Delta\tilde{f}) \triangleq \left| \sum_{i=1}^{N} r_i e^{-j2\pi \Delta\tilde{f} i T_s} \right|^2 = \sum_{l=1}^{N} \sum_{m=1}^{N} r_l r_m^* e^{-j2\pi \Delta\tilde{f} T_s (l-m)} \quad (1.20)$$

Taking the derivative with respect to Δf and equating it to zero we find the maximum as the solution of

$$\sum_{k=1}^{N}\sum_{m=1}^{N}(k-m)r_k r_m^{*}e^{-j2\pi\Delta\hat{f}T_s(k-m)}=0 \qquad (1.21)$$

Rearranging a few terms yields

$$\mathrm{Im}\left\{\sum_{k=1}^{N-1}k(N-k)R(k)e^{-j2\pi\Delta\hat{f}kT_s}\right\}=0 \quad \text{where:} \quad R(k)\triangleq\frac{1}{N-k}\sum_{i=k+1}^{N}r_i r_{i-k}^{*},\ 0\le k\le N-1 \qquad (1.22)$$

To avoid "false peaks" the operating range of the estimator is limited by a windowing function. This accounts for the fact that at k=0 the autocorrelation bears little information about the offset and at the k=N the R(k) is a poor estimate of the offset. This allows the estimate to be written in the following way.

$$\mathrm{Im}\left\{\sum_{k=1}^{M}R(k)e^{-j2\pi\Delta\hat{f}kT_s}\right\}=0. \qquad (1.23)$$

In order to approximately solve (1.23) a taylor series approximation is used for the entire expression to yield

$$\Delta\hat{f}\cong\frac{1}{2\pi T_s}\frac{\sum_{k=1}^{M}\mathrm{Im}\{R(k)\}}{\sum_{k=1}^{M}k\,\mathrm{Re}\{R(k)\}} \qquad (1.24)$$

Next we use the approximation $R(k) = e^{j(2\pi\Delta fkTs)} + n_k \approx 1 + j(2\pi\Delta fkTs) + n_k$ to obtain (assuming $|n_k| << 1$)

$$\sum_{k=1}^{M} \mathrm{Im}\{R(k)\} \equiv M \arg\left\{\sum_{k=1}^{M} R(k)\right\} \qquad (1.25)$$

$$\sum_{k=1}^{M} k\,\mathrm{Re}\{R(k)\} \equiv \frac{M(M+1)}{2} \qquad (1.26)$$

Finally our maximum likely estimate for Δf is given by the following equation [6]:

$$\Delta\hat{f} \equiv \frac{1}{\pi T_s (M+1)} \arg\left\{\sum_{k=1}^{M} R(k)\right\} \qquad (1.27)$$

The diagram in Figure 6 illustrates the Matlab implementation of a software AFC circuit. The maximum likelihood estimate referenced above as equation 1.27 is used to estimate the frequency offset of the incoming digital samples. The estimate is then passed to a simple first order loop filter show in equation 1.28 that keeps the estimates from diverging by utilizing an update step γ in

$$\delta\hat{f}_i = \delta\hat{f}_{i-1} - \gamma\Delta\hat{f}_{i-1} \qquad (1.28)$$

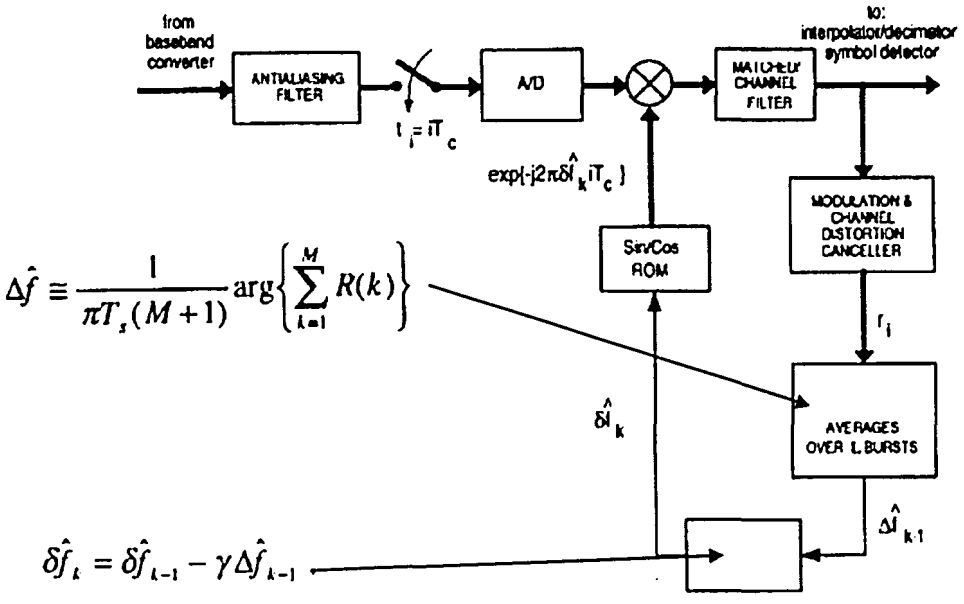

Figure 6: Software AFC circuit for carrier offset.

The graph in Figure 7 plots the theoretical limitations of the AFC estimator. As derived from the graph below the maximum frequency offset normalized to the sampling period that can be linearly predicted reliably with this circuit is about 0.002. This means that to find the maximum amount of frequency offset the product of the sampling frequency and the 0.002 bound must be taken. In the testbed, the Comblock modules have a sampling frequency of 40MHz, which allow us to correct for 80KHz of carrier frequency offset with this AFC.

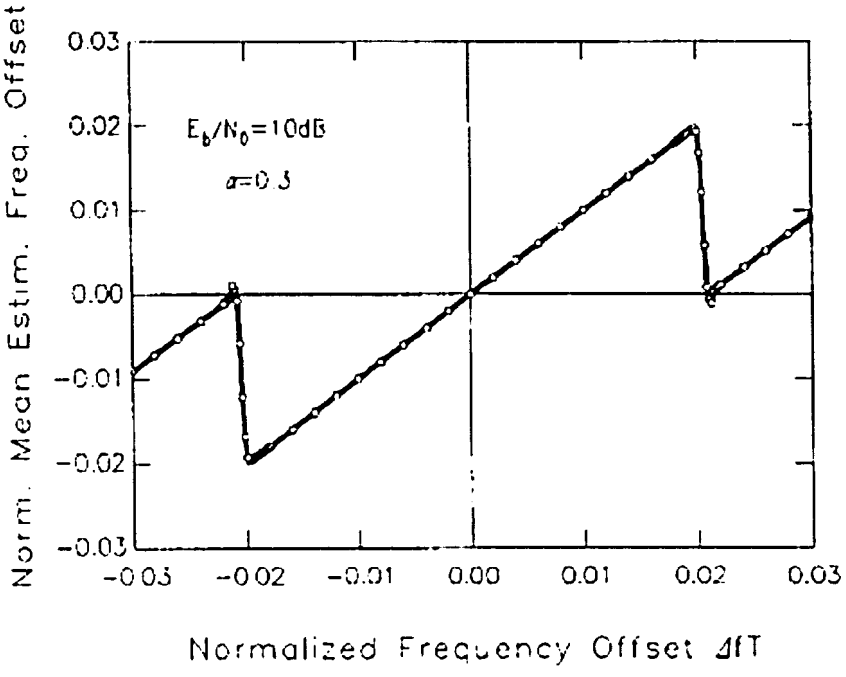

Figure 7: Estimate bound for the AFC circuit [2].

B. Channel Estimation:

The following approach was used to extract the channel estimates from the orthogonal pilot sequences. If we assume the receive signal is r_j and the amplitude energy of the pilot is A. Then by using the fact that the two pilot sequences P_1 and P_2 are orthogonal it can be shown that the Minimum Mean Square Error (MMSE) estimate of h_{ij} is given by [4] [7] [8].

$$\hat{h}_{i,j} = \frac{P_i(n) * r_j(n)}{A\|P_i(n)\|^2} \quad (1.28)$$

Where $\hat{h}_{i,j}$ is an estimate on h_{ij} and e_{ij} is the estimation error in

$$\hat{h}_{i,j} = h_{ij} + e_{ij} \quad (1.29)$$

The estimation error can be represented by

$$e_{ij} = \frac{P_i(n)^* n_j(n)}{A\|P_i(n)\|^2} \quad (1.30)$$

Since channel estimation can only be preformed during the time slots of the pilot sequences, the newly obtain estimates will have to be interpolated to the other time slots containing data. You can easily see the correspondence to the sampling theorem. Namely increasing the number of pilot sequences inserted will increase the accuracy of the estimation. However as more pilots sequences are added to the transmit frame, the amount of data that can be inserted in the transmit frame decreases which lowers the throughput. In this testbed, a lowpass Gaussian filter was used to average the channel estimates and provide a stable channel interpolation. [4].

C. Transmitter Processing:

The baseband signals were created by encoding a random bit steam which represents wireless network data, with the Alamouti STBC. The Alamouti encoder will separate out two individual transmit codes from the single bit stream. Then two 13 bit orthogonal pilot sequences were added to each of the two transmit sequences for synchronization and channel estimation. The 13 bit barker code was chosen for the two pilot sequences because the code has great autocorrelation properties. Namely the coding gain of the barker used in this implementation is 13. [1] Finally the two sequences are upconverted and channel coded by the raised cosine filter. The entire waveform is up-sampled eight times in order to make sure no data is totally lost. After the signals are successfully

coded, the bits are formatted so that they can be properly streamed though the COMblock's 20-bit connectors. The transmitter code writes two binary files, which are then uploaded to both transmitter assemblies. This is done by connecting over the TCP/IP network to both COM-5001 LAN/IP Interfaces each at separate IP addresses, through the COMblock Control Center. The COM-5001 modules act as a gateway to the two transmitters. Once the data is successfully loaded onto the COM-8001's memory, transmission can begin. To transmit, the Control Center is used to begin a continuous download from the COM-8001 at 40 Msample. These signals are passed onto both COM-2001 for Dual D/A conversion and are finally modulated with a 2.4 GHz carrier once the analog stream reaches each of the COM-4001 Quadrature Modulator. In order to keep synchronization offset to a minimum a common clock is shared between the two transmitter arrays.

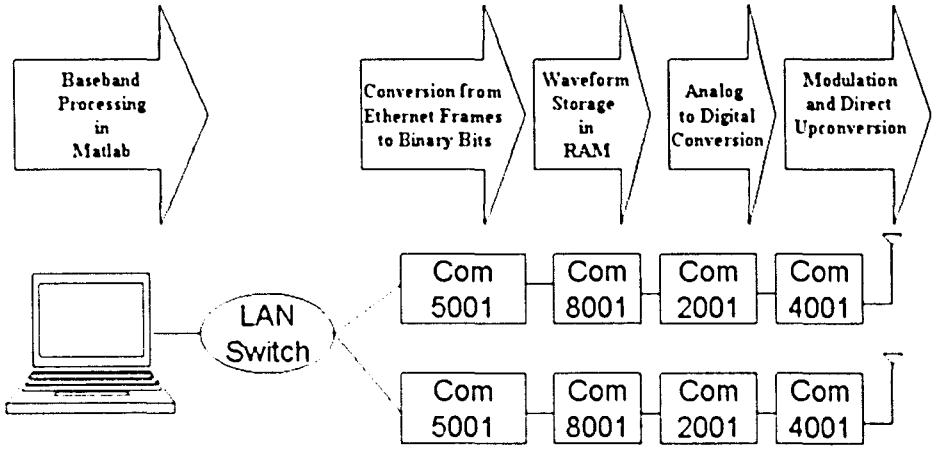

Figure 8: Block Diagram of Transmitter Configuration.

D. Receiver Processing:

In order to capture the STBC signals, two more COMblock Control Center sessions must be opened. Connections to both receiver assemblies are achieved through each receiver's COM-5001 Lan/IP interface. Once the assemblies are recognized, both COM-8002 Data Acquisition COMblock modules can be set to upload each of the receive signals from the two antennas. The upload windows are set to be three-times the length of the actual transmitted waveform. This was done in order to make sure that none of the transmitted waveforms were missed. Once the captured waveforms have been uploaded to both COM-8002 modules, they can be downloaded as binary files to a PC for further signal processing. Here again both receivers are triggered from a common clock to prevent timing offsets.

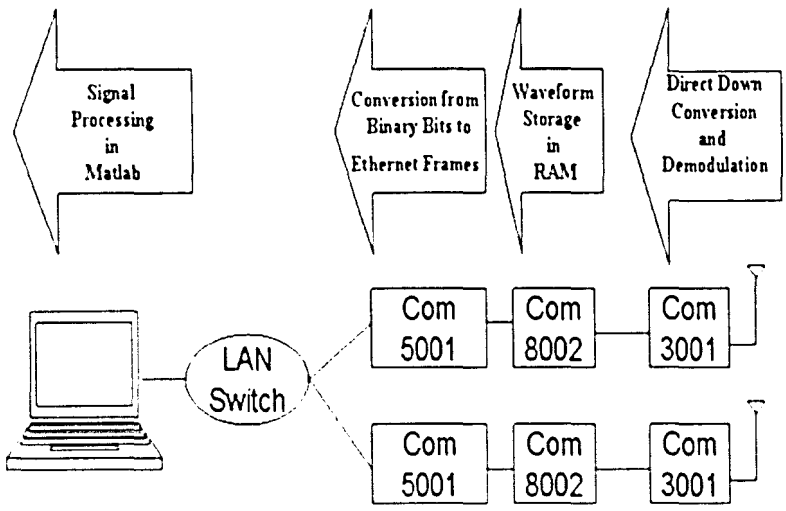

Figure 9: Block Diagram of Receiver configuration.

E. Matlab Processing

Matlab was used as the signal processing tool that provided a way to process the digital samples for carrier and timing offsets in software. The digital samples were first passed to the AFC function in figure 6. The samples were next time synchronized by correlating the received signals with the two orthogonal 13 bit barker pilot sequences, the same sequences that were used on each transmitter. When plotting the absolute values of the correlated data points, we see a peak where the time synchronization sequences match. We can now assume that the transmitted data starts after the point in time where the peak occurs. Now we can collect the same length of data points that was transmitted, this length is the length of the transmitted data that has been upsampled by 8. Once we collect these points we downsample 8 times to get a data signal and two pilot sequences. The pilot symbols are passed next to the channel estimation and interpolation function. This function will provide the interpolated estimate of the channel per each received signal sample. The sampled signal and the channel estimate are then passed to the MRRC function that will present a signal projection to the ML detector for decoding. The decoded bits are then compared to the transmitted bits to establish a BER curve.

V. Conclusion

Overall we have proved that a flexible MIMO testbed can be built and run successfully. The following graphs give us a picture of the indoor wireless channel and the capacity gain one could achieve in such an environment. Figure 10 and 11 present the actual

measurements from the MIMO STBC testbed. Figure 10 shows the channel gains of the MIMO channel estimates over time. From the arrangement of the array, the estimated channel envelope profiles as shown in Figure 10, reveal that the environment is stationary and that the order of the MIMO channel estimates follows the following pattern: $| h_{22} | > | h_{21} | > | h_{12} | > | h_{11} |$. That is, the channel gains from transmit antenna 2 are stronger than the corresponding gains from transmit antenna 1. Figure 11 shows that we are getting approximately two times the improvement in capacity using MIMO than if we were to use any of the channels separately.

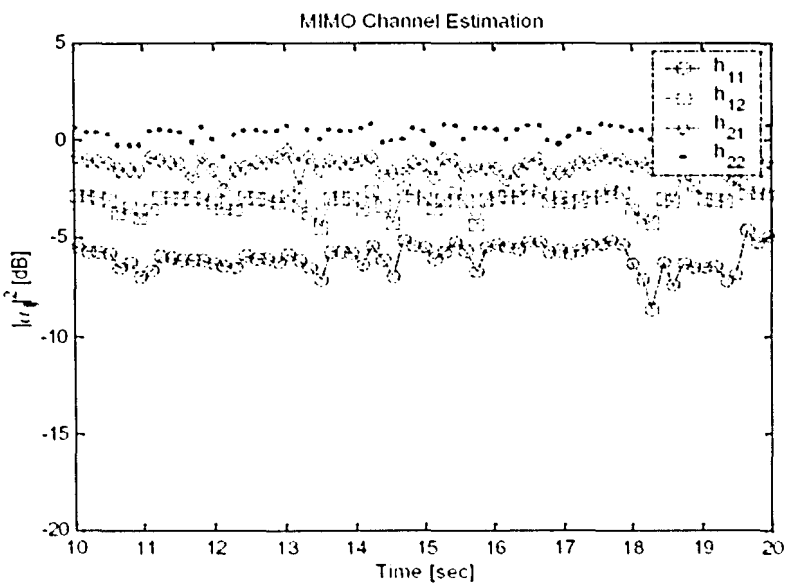

Figure 10: Channel gain plotted over a 20 second time window.

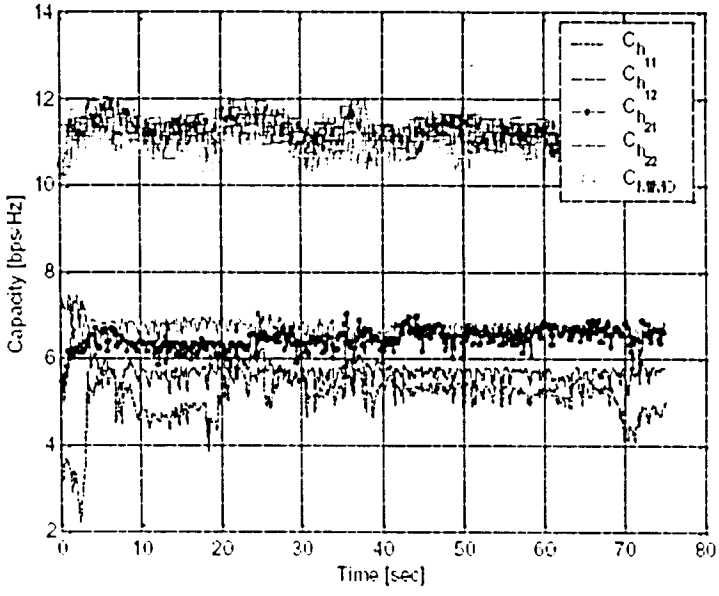

Figure 11: Throughput of MIMO channel over an eighty second time window for the experimental testbed.

VI. Appendix

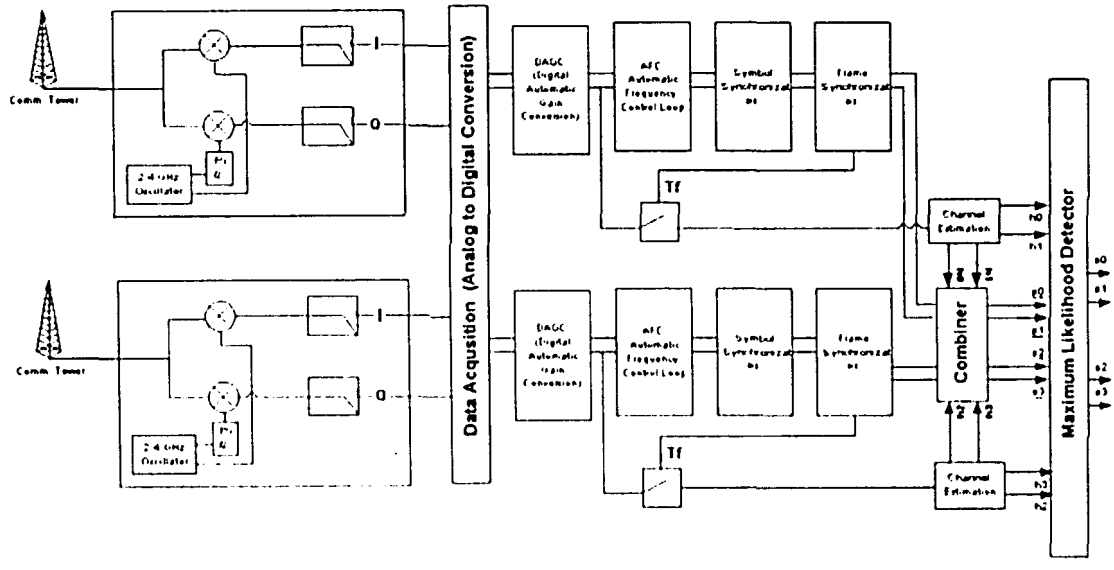

Figure 12: Flow chart of the Receiver Architecture

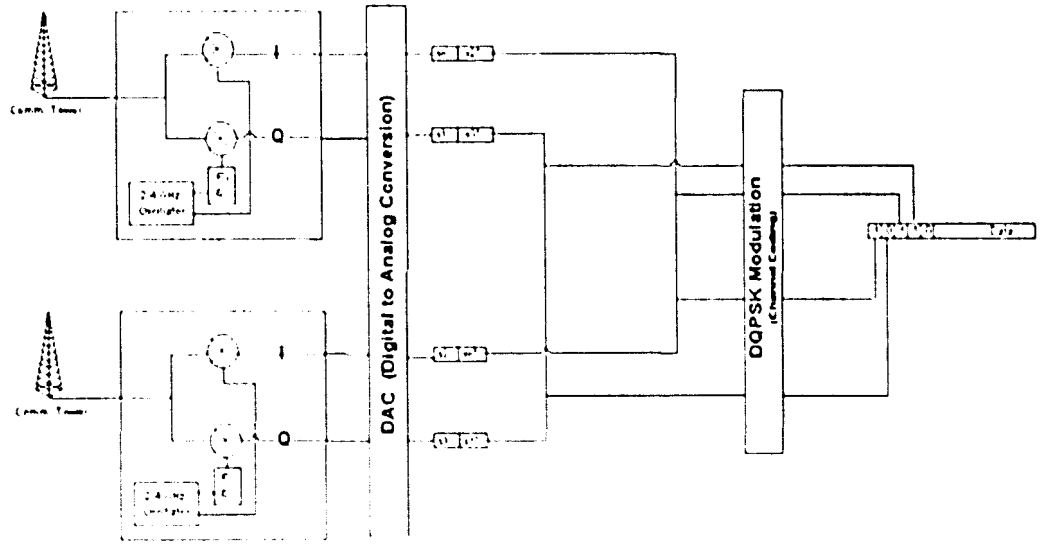

Figure 13: Flow chart of the Transmitter Architecture

VII. References:

[1] M. Skolink, Radar Handbook. 2nd edition. New York: McGraw-Hill, 1990.

[2] J. Prokais, *Digital Communications*. 4th edition. New York: McGraw-Hill, 2001.

[3] S. Alamouti, "A simple transmit diversity technique for wireless communications," IEEE Journal On Selected Areas in Communications, vol.1 6, pp.1 45 1-1 458, Oct. 1998.

[4] S. Sampei and T. Sunaga, "Rayleigh fading compensation method for 16 QAM in digital land mobile radio channels," in *Proc. IEEE VTC'89*, San Francisco, CA, May 1989, vol. I, pp. 640–646.

[5] V. Tarokh, N. Seshadri, and A. R. Calderbank, "A Space–Time Coding Modem for High-Data-Rate Wireless Communications," IEEE Journal On Selected Areas in Communication, Vol. 16, No. 8, October, 1998

[6] H. Meyr, M. Moeneclaey, S Fechtel, "Digital Communication Receivers", New York: John Wiley & Sons, 1998

[7] J. K. Cavers, "An analysis of pilot symbol assisted modulation for Rayleigh faded channels," *IEEE Trans. Veh. Technol.*, vol. 40, pp. 683–693, Nov. 1991.

[8] D. Samardzija and N. Mandayam "Pilot-Assisted Estimation of MIMO Fading Channel Response and Achievable Data Rates", IEEE Transactions on Signal Processing, VOL. 51, NO. 11, November, 2003.

VIII. Vita

Albert J. Davis

Albert Davis was born in Ashland, PA on January 1, 1977 to Dwight and Mary Davis. In May of 1999 he graduated from Lehigh University with a Bachelor of Science Degree in Electrical Engineering. He worked for Accenture (formally Anderson Consulting) in the telecommunication consulting division with clients that included AT&T and IBM from June 1999 till August 2002. Albert entered graduate school at Lehigh University full time in August 2002 to purse a doctorate degree in Electrical Engineering. During the years of 2002 and 2003 he was a teaching assistant for the Electrical and Computer Engineering Department as well as a research assistant to Professor Rick Blum. In January of 2004, Albert began working for Lockheed Martin's Advanced Technology Lab in Cherry Hill, NJ. He is pursing his doctorate research part time at Lehigh University under the support of Lockheed Martin in the field of RF communications and signal processing. He presently resides in Cherry Hill, NJ with his wife Renee.

END OF TITLE